

# Accurate detection of melanoma skin cancer using fuzzy based SegNet model and normalized stacked LSTM network

Woothukadu Thirumaran Chembian<sup>1</sup>, Krishna Murthi Sankar<sup>2</sup>, Seerangan Koteeswaran<sup>3</sup>,  
Kandasamy Thinakaran<sup>4</sup>, Periyannan Raman<sup>5</sup>

<sup>1</sup>Department of Computer Science and Engineering, Vel Tech High Tech Dr. Rangarajan Dr. Sakunthala Engineering College (Autonomous), Chennai, India

<sup>2</sup>Department of CSE-ET, CVR College of Engineering, Telangana, India

<sup>3</sup>Department of CSE (Artificial Intelligence and Machine Learning), S.A. Engineering College (Autonomous), Chennai, India

<sup>4</sup>Department of Computer Science and Engineering, Saveetha Institute of Medical and Technical Sciences, Saveetha University, Chennai, India

<sup>5</sup>Department of Management Studies, Panimalar Engineering College, Chennai, India

## Article Info

### Article history:

Received Jan 19, 2024

Revised Feb 29, 2024

Accepted Mar 18, 2024

### Keywords:

Deep fuzzy clustering

LSTM

Melanoma skin cancer

ResNet-50

SegNet

## ABSTRACT

Early detection of melanoma skin cancer (MSC) is critical in order to prevent deaths from fatal skin cancer. Even though the modern research methods are effective in identifying and detecting skin cancer, it is a challenging task due to a higher level of color similarity between melanoma non-affected areas and affected areas, and a lower contrast between the skin portions and melanoma moles. For highlighting the aforementioned problems, an efficient automated system is proposed for an early diagnosis of MSC. Firstly, dermoscopic images are collected from two benchmark datasets namely, international skin imaging collaboration (ISIC)-2017 and PH2. Next, skin lesions are segmented from dermoscopic images by implementing a fuzzy based SegNet model which is a combination of both deep fuzzy clustering algorithm and the SegNet model. Then, hybrid feature extraction (ResNet-50 model and local tri-directional pattern (LTriDP) descriptor) is performed to capture the features from segmented skin lesions. These features are given into the normalized stacked long short-term memory (LSTM) network to categorize the classes of skin lesions. The empirical evaluation reveals that the proposed normalized stacked LSTM network achieves 98.98% and 98.97% of accuracy respectively on the ISIC-2017 and PH2 datasets, and these outcomes are more impressive than those of the conventional detection models.

*This is an open access article under the [CC BY-SA](https://creativecommons.org/licenses/by-sa/4.0/) license.*



## Corresponding Author:

Woothukadu Thirumaran Chembian

Department of Computer Science and Engineering, Vel Tech High Tech Dr. Rangarajan Dr. Sakunthala Engineering College (Autonomous)

Chennai, India

Email: wtchembian@velhightech.com

## 1. INTRODUCTION

In recent decades, melanoma skin cancer (MSC) has become a serious and prevalent health disorder with a high mortality rate. Both malignant and benign skin cancers occur due to the damage caused in deoxyribonucleic acid [1]. A high exposure to ultraviolet radiation causes this damage, and leads to unregulated and excessive growth of cells. The benign skin cancers (cysts, seborrheic keratosis, dermatofibromas, cherry angiomas, skin tags, and pyogenic granulomas) do not spread, whereas malignant skin cancers are uncontrollable and spread throughout the human body [2], [3]. There is a chance of curing

malignant skin cancers when detected at an early stage. However, MSC detection at an early stage is a difficult process; therefore, several methods are developed for detecting and classifying the MSC [4], [5]. Recently, numerous segmentation algorithms are developed for automatic skin lesion segmentation such as, region growing, edge detection, and thresholding [6]. Furthermore, several handcrafted feature extraction techniques are used to extract image properties like color, texture and shape. The traditional techniques have a high semantic gap among extracted features, further leading to the curse of the dimensionality problem [7]. Even though the conventional machine and deep learning models offer adequate outcomes, they are ineffective in achieving satisfactory results, especially when the dataset is limited [8]. The existing researches related to “MSC detection” are surveyed as follows. Araújo *et al.* [9] integrated Link-Net and U-Net models for melanoma region segmentation. Further, fine-tuning and transfer-learning techniques were utilized for learning the properties of the disease. The simulation experiments carried out on the DermIS, ISIC-2018, and PH2 datasets showed the superiority of this hybrid segmentation model. Ahmed *et al.* [10] combined mask region based convolutional neural network (RCNN) and Retina-Net models for automatic segmentation and detection of melanoma lesions. The generalization capability of this hybrid segmentation model was evaluated utilizing PH2 and ISIC-2018 datasets. The outcomes revealed that this hybrid segmentation model achieved better segmentation performance, even in the presence of occlusion changes (poor color contrast, and variations in geometrical size and shape). In comparison to traditional detection models, the hybrid deep learning-based segmentation model showed better accuracy improvement. Even though the modern research methods were effective in identifying and detecting skin cancer, it was still challenging due to higher level of color similarities between melanoma non-affected areas and the affected areas, and a lower contrast between the skin portions and melanoma moles.

Thanh *et al.* [11] presented a novel framework for automatic MSC detection utilizing different image processing techniques. This framework comprised three important phases namely, pre-processing by adaptive principal curvature (APC) for removing hairs in dermoscopic images, skin lesion segmentation by color normalization that efficiently discriminated skin lesions from the skin tone, alongside the necessary feature information being extracted using asymmetry-border-colour-diameter (ABCD) rule for evaluating the score of skin lesions in order to detect and segment melanoma. An online benchmark dataset (ISIC-2017) was used to validate the success of this framework. Nawaz *et al.* [12] firstly employed a faster RCNN model for enhancing the visual information, alongside eliminating noise and illumination problems in dermoscopic images. Then, the melanoma skin lesions with variable boundaries and sizes were segmented by applying the fuzzy K-means (FKM) clustering algorithm. The performance of this presented framework was validated on ISIC-2017 dataset, and the outcomes showed that this framework superiorly outperformed the existing frameworks in the context of MSC detection. Furthermore, Saba [13] performed MSC detection utilizing non-handcrafted and handcrafted features. The clinical features called Gabor filters, asymmetry, visual textures, Markov random fields, Menzies method, local binary patterns (LBP), border color, border diameter, seven-point detection, oriental histography, and fractal dimension were explored for MSC detection. These captured features were passed into the conventional machine learning models: random forest, Adaboost, K-nearest neighbour (KNN) and support vector machine (SVM) to classify the stages of MSC into benign, suspicious, and malignant. Several evaluation measures including specificity, sensitivity, precision, dice coefficient, accuracy, and Jaccard index were utilized for assessing the effectiveness of the reported models.

Al-Masni *et al.* [14] introduced a full-resolution convolutional network (FrCN) for precise segmentation of skin lesion boundaries. Next, the skin lesions were classified by employing the CNN models: DenseNet-201, Inception-ResNet-v2, ResNet-50, and Inception-v3. This presented deep learning based framework was validated on three online datasets (ISIC-2018, 2017, and 2016) using the evaluation measures of sensitivity, F1-score, accuracy, and specificity. Goyal *et al.* [15] developed an automated framework through the ensemble of different deep learning models for accurate segmentation and detection of skin lesions in dermoscopic images. Additionally, color normalization was performed to remove hair follicles in the dermoscopic images. This framework’s (incorporation of DeeplabV3+ and mask RCNN models) performance was tested on two benchmark datasets, PH2 and ISIC-2017. By surveying the existing literature, the following few problems are needed to be addressed in this present study for precise segmentation and classification of MSC. In this context, the conventional classification models which are, random forest, Adaboost, KNN, and SVM have two major concerns of overfitting and outliers. In addition, the performing of experiments by using only the non-handcrafted and handcrafted features increases the semantic gap among features and results in a poor classification performance. Furthermore, the incorporation of two or three pre-trained deep learning models was computationally complex and required a high-end computer for processing an enormous amount of image data. In order to counter the above-described problems, an efficient automated system is proposed for MSC detection in this study. The contributions of this study are given:

- A fuzzy based SegNet model is implemented for precise segmentation of skin lesions on the ISIC-2017 and PH2 datasets. Hybrid feature extraction is performed using the ResNet-50 model and LTriDP descriptor for extracting most informative deep features from the segmented skin lesion regions.
- A normalized stacked long short term memory (LSTM) network is proposed for classifying the following three classes, melanoma, seborrheic keratosis, and benign on the ISIC-2017 dataset, alongside the classes, melanoma, atypical nevi, and common nevi on the PH2 dataset. Six evaluation measures are used to analyse the performance of both fuzzy based SegNet model and the normalized stacked LSTM network.

The remaining sections of the manuscript are arranged in following format; section 2 provides information of the proposed methodology. Section 3 provides results, discussion and comparison of the proposed method, while section 4 provides conclusion of research.

## 2. METHODS

In the context of MSC segmentation and classification, the proposed automated system includes four steps. At first, the dermoscopic images are acquired from two benchmark datasets, ISIC-2017 and PH2. Next, the skin lesions are accurately segmented by implementing a fuzzy based SegNet model; and further, in the segmented images, features are extracted by incorporating the LTriDP descriptor and ResNet-50 model. Lastly, the obtained features are fed into the normalized stacked LSTM network for classifying the types of skin lesions. The steps involved in this automated system are visually described in Figure 1.

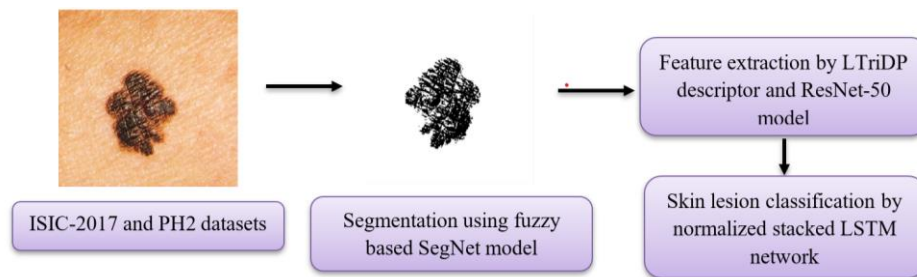


Figure 1. Steps involved in this automated system

### 2.1. Dataset description

The fuzzy-based SegNet model and the normalized stacked LSTM networks’ performance are analysed on two benchmark datasets, ISIC-2017 and PH2. Firstly, the ISIC-2017 dataset comprises 2,750 dermoscopic images belonging to three classes (melanoma, seborrheic keratosis, and benign). This ISIC-2017 dataset has 600 images in test-set, 150 images in validation-set, and 2,000 images in the training-set [16]. The data distribution of the ISIC-2017 dataset is presented in Table 1.

Table 1. Data distribution of the ISIC-2017 dataset

Classes	Test-set	Validation-set	Training-set
Melanoma	117	30	374
Seborrheic keratosis	90	42	254
Benign	393	78	1,372

On the other hand, PH2 dataset encompasses 200 dermoscopic images with a pixel resolution of  $768 \times 560$ . Among the 200 images, 40 images are melanoma, 80 images are atypical nevi, and the remaining 80 images are common nevi [17]. This PH2 dataset has a medical annotation for all dermoscopic images which include, histological and clinical diagnosis, assessment of many dermoscopic criteria (blue-whitish veil, regression areas, streaks, globules/dots, pigment network, and color), and medical segmentation of the skin lesions. The dermoscopic images of ISIC-2017 and PH2 datasets are pictorially represented in Figure 2. Figure 2(a) represents the sample images from ISIC-2017 dataset and Figure 2(b) represents the sample images from PH2 dataset.

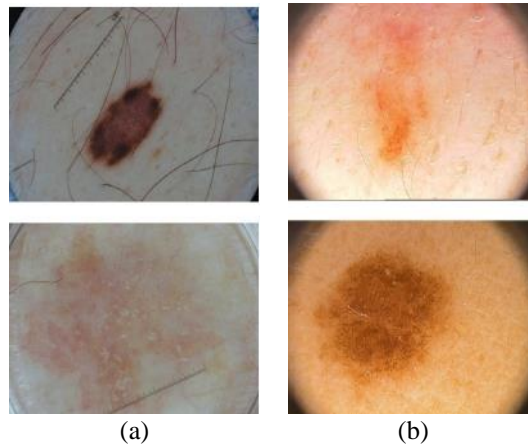


Figure 2. Dermoscopic images (a) ISIC-2017 dataset and (b) PH2 dataset

## 2.2. Skin lesion segmentation

After acquiring the dermoscopic images from ISIC-2017 and PH2 datasets, the skin lesions are accurately segmented by deploying a fuzzy based SegNet model. This segmentation model is an incorporation of deep fuzzy clustering algorithm and SegNet model. In this scenario, the deep fuzzy clustering algorithm and SegNet model are incorporated on the basis of the cross entropy loss function. The acquired dermoscopic images from ISIC-2017 and PH2 datasets are considered as the input for deep fuzzy clustering algorithm which is represented as  $C = \{C_1, \dots, C_i, \dots, C_n\}$ , and  $n$  denotes the number of dermoscopic images. In this clustering algorithm, the batch size is denoted as  $f_t$ , maximum number of iterations is denoted as  $Z_{max}$ , and the cluster amount is indicated as  $M$ . A sample dermoscopic image is considered as  $C_i$ , divided into  $\frac{f}{f_t}$  batches and further, every batch of the training data is found with  $C_s, s = 1, 2, \dots, \frac{f}{f_t}$ . In order to predict the affinities  $X \in \mathcal{R}^{f_t \times f_t}$ , the pseudo labels are  $\gamma_s$ , fuzzy membership is  $P_s$ , and the hidden features  $T_s$  are computed for every batch. Then, the hidden features  $T_s$  and reconstruction error  $N_{y,z}(C_s)$  are calculated for each batch amount. The auto-encoder's objective function  $O(C, \theta)$  is mathematically presented in (1).

$$O(C, \theta) = \frac{1}{n} \sum_{i=1}^n \|N_{y,z}(C_i) - C_i\|^2 + \gamma \times reg(\gamma) \quad (1)$$

Where, the regularization expression is represented as  $reg(\gamma)$  and the euclidean standard is stated as  $\|\cdot\|$ . In this context, the regularization expression  $reg(\gamma)$  solves the issue of overfitting. Furthermore, the Kullback-Leibler (KL) divergence based objective function  $K_s$ , target  $X_s$ , and fuzzy membership  $P_s$  is computed. The coefficient  $\gamma$  is used for controlling the scale of KL-divergence. Further, the graph regularization  $v_o$  is calculated by using  $T_s$  and  $K_s$ , and is mathematically depicted in (2).

$$\min v_o = \min \sum_{i,\rho=1}^n \|o_i - o_\rho\|^2 K_{i,\rho} \quad (2)$$

Where,  $K_{i,\rho}$  is the affinity between  $K_\rho$  and  $K_i$ . In this clustering algorithm, the loss function  $FL$  is formulated using (3). Additionally, the clustered pattern is mathematically denoted in (4). Where, the desired target is denoted as  $I_{ij}$ , the degree of membership or belongingness for  $C_i$  is denoted as  $H_{ij}$ , the trained weights of the clustering layer are denoted as  $\mu_1$  and  $\mu_2$ , total sequence patterns are indicated as  $m$ , grouped patterns are represented as  $P$ , and the output of this clustering algorithm is denoted as  $N_i$  which is combined with the SegNet model for skin lesion segmentation.

$$FL = \sum_{i=1}^n \|N_{y,z}(C_i) - C_i\|^2 + \mu_1 \sum_{i=1}^n \sum_{j=1}^m I_{ij} \log \frac{I_{ij}}{H_{ij}} + \mu_2 \sum_{i,\rho=1}^n \|o_i - o_\rho\|^2 K_{i,\rho} \quad (3)$$

$$P = \{P_1, P_2, \dots, P_m\} \quad (4)$$

The SegNet is a deep-learning based segmentation model, which encompasses an encoder network, a decoder network, and a pixel-wise classification layer [18], [19]. The encoder network has thirteen

convolutional layers for encoding the input data and is inspired from the concept of visual geometry group (VGG)-16 model. Next, the decoder network maps the lower-resolution encoder feature maps for pixel-wise classification. In this model, the decoder network utilizes the pooling indices for performing non-linear upsampling. This process eliminates the necessity of learning to perform upsampling. The up-sampled maps are sparse and integrated with the trainable filter for generating dense feature maps. In the context of skin lesion segmentation, the output of the SegNet model is denoted as  $SN_i$ . As mentioned earlier, a cross entropy loss function is utilized in this fuzzy based SegNet model for combining the output of both SegNet model and deep fuzzy clustering algorithm. This process  $G_i$  is mathematically expressed in (5). Where, cross entropy loss consequent to clustering algorithm output  $N_i$  is represented as  $\eta_1$  and cross entropy loss corresponding to SegNet model output  $SN_i$  is denoted as  $\eta_2$ . The output of this fuzzy based SegNet model is pictorially presented in Figure 3. The Figure 3(a) represents segmented dermoscopic images from ISIC-2017 dataset and Figure 3(b) represents segmented dermoscopic images from PH2 dataset.

$$G_i = \eta_1 N_i + (1 - \eta_2) SN_i \tag{5}$$

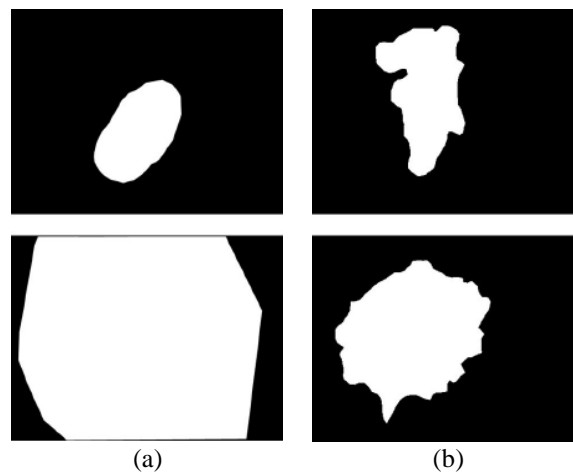


Figure 3. Segmented dermoscopic images (a) ISIC-2017 dataset and (b) PH2 dataset

### 2.3. Feature extraction

Following the segmentation of skin lesions, hybrid feature extraction (ResNet-50 model and LTriDP descriptor) is presented in this section. The ResNet-50 model comprises 49 convolutional layers and one fully connected layer for extracting features from the segmented skin lesion regions [20]–[22]. The output size of the ResNet-50 model is 2048; here,  $NL_{ResNet}$  represents the non-linear function of the ResNet-50 model, and  $ResNet_{i,j}$  indicates the features extracted from  $GreyPixel_{i,j} = 1,2,3, \dots, 2048$ . The feature extraction process of the ResNet-50 model is mathematically denoted in (6).

$$ResNet_{i,j} = NL_{ResNet}(GreyPixel_i) \tag{6}$$

The LTriDP descriptor is an extended version of the LBP descriptor which has a relationship with the neighbourhood pixels in all directions [23]. In a specific radius, every center pixel has eight neighbourhood pixels, and in the next radius, there are sixteen neighbourhood pixels, and so on. The limited number of neighbourhood pixels provides more information when they are closer to the center pixel. In this scenario, the eight neighbourhood pixels are considered for creating the patterns. The LTriDP descriptor utilizes the relationship among adjacent neighbors with neighboring pixels, and the relationship of neighboring pixel with center pixel. One-neighbourhood pixels and its two adjacent pixels (either horizontal or vertical pixels) are compared with the center pixel, as graphically presented in Figure 4. The output of the LTriDP descriptor  $Fe_{LTriDP}$  is mathematically expressed in (7). Here, a feature level fusion is carried out for combining 2048 feature vectors of the ResNet-50 model, and 4982 feature vectors of LTriDP descriptor which are lastly passed to the normalized stacked LSTM network for skin lesion classification.

$$Fe_{LTriDP} = \{LTriDP_{1 \times 1}, LTriDP_{1 \times 2}, \dots, LTriDP_{1 \times 4982}\} \tag{7}$$

4	7	9
2	6	8
7	2	9

Figure 4. Sample notation of center and neighbourhood pixels

#### 2.4. Skin lesion classification

The extracted features from the ResNet-50 model and LTriDP descriptor are given into the normalized stacked LSTM network for classifying the types of skin lesions. The stacked LSTM network is an improved version of the LSTM network because the LSTM network comprises a single hidden layer, while the stacked LSTM network comprises multiple hidden layers [24]–[26]. By stacking the multiple hidden layers, the network gets deeper and captures longer-term spatial and temporal information from the extracted features. This process improves the classification performance, particularly, in the context of MSC detection. In the proposed normalized stacked LSTM network, a normalization layer is added to every LSTM layer in the network. The inclusion of the normalization layer reduces internal covariate shift problem as well as the risk of overfitting, thereby speeding up and stabilizing the training process. In medical imaging application, the stacked LSTM network is more prone to exploding and vanishing gradient problems. This normalization process reduces these problems by effectively maintaining activations (sigmoid and tangent) in a specific scale [27], [28]. During the back-propagation process, the normalization simplifies the propagation of gradients. The parameters considered in the normalized stacked LSTM network are: optimizer is Adam, batch size is 32, total hidden units in every layer is 50, total epochs is 100, learning rate is 0.001, and length of time lags is 15. The empirical evaluation of the fuzzy based SegNet model and the normalized stacked LSTM network are depicted in section 4. The architecture of the normalized stacked LSTM network is stated in Figure 5.

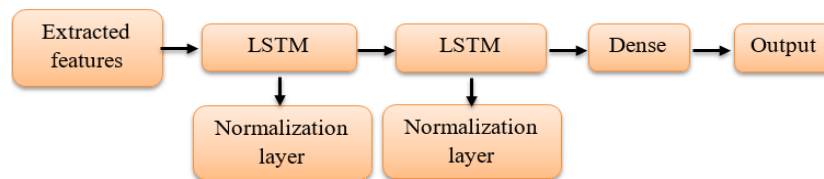


Figure 5. Architecture of the normalized stacked LSTM network

### 3. RESULTS

The fuzzy based SegNet model and the normalized stacked LSTM network are implemented utilizing MATLAB R2020b (version 9.9) software. This proposed system is executed on a computer equipped with windows 11 (64-bit) operating system, 2TB hard-drive, Intel i7 processor, and 16GB memory. Two online benchmark datasets, ISIC-2017 and PH2 are utilized for investigating the performance of both fuzzy based SegNet model and normalized stacked LSTM network. The evaluation measures, jaccard coefficient and dice coefficient are utilized to analyse the performance of the fuzzy based SegNet model. On the other hand, the evaluation measures: accuracy, sensitivity, precision, and matthews correlation coefficient (MCC) are utilized to investigate the performance of the normalized stacked LSTM network in the context of MSC detection.

#### 3.1. Evaluation measures

In this medical imaging application, Jaccard coefficient and dice coefficient are effective in estimating the similarity between two sets  $A$  and  $B$ , where,  $A$  denote skin lesions that are detected by a fuzzy based SegNet model and  $B$  represents the ground-truth regions. The formulas used to calculate jaccard coefficient and dice coefficient are illustrated in (8) and (9).

$$\text{Jaccard coefficient} = \frac{|A \cap B|}{|A \cup B|} \quad (8)$$

$$Dice\ coefficient = \frac{2|A \cap B|}{|A| + |B|} \tag{9}$$

In this context of MSC detection, accuracy is defined as the percentage of precisely determined cases (true negative (TN) and true positive (TP)) to the total cases. Furthermore, sensitivity estimates the ability of a normalized stacked LSTM network for correctly identifying the positive instances. Specifically, sensitivity is defined as the percentage of actual melanoma cases precisely determined by the normalized stacked LSTM network. The mathematical formulas used to compute accuracy and sensitivity are specified in (10) and (11).

$$Accuracy = \frac{TP + TN}{TP + TN + FP + FN} \times 100 \tag{10}$$

$$Sensitivity = \frac{TP}{TP + FN} \times 100 \tag{11}$$

MCC is one of the efficient evaluation measures in image classification which considers TN, TP, false negative (FN), and false positive (FP) cases. This evaluation measure is useful, particularly when dealing with imbalanced image datasets. The evaluation measure ‘precision’ estimates the accuracy of positive prediction done by the proposed normalized stacked LSTM network. The numerical expressions of precision and MCC are denoted in (12) and (13).

$$Precision = \frac{TP}{TP + FP} \times 100 \tag{12}$$

$$MCC = \frac{TP \times TN - FP \times FN}{\sqrt{(TN + FN)(TN + FP)(TP + FN)(TP + FP)}} \times 100 \tag{13}$$

**3.2. Quantitative analysis**

As represented in Table 2, in the context of MSC detection, the fuzzy based SegNet model is compared with five conventional segmentation models: K-means clustering, fuzzy C means clustering, U-Net, and SegNet using two evaluation measures (Jaccard coefficient and dice coefficient). By viewing Table 2, it is evident that the fuzzy based SegNet model obtains impressive segmentation results with 0.98 and 0.97 of Jaccard coefficient, and 0.99 and 0.98 of dice coefficient on the ISIC-2017 and PH2 datasets, respectively. Generally, skin lesions vary in size, shape, and appearance. This fuzzy based SegNet model is robust and flexible in managing the gradual transitions between different types of tissues. The lesions with fuzzy boundaries are useful in differentiating abnormal and normal tissues. Moreover, the raw dermoscopic images often contain artifacts and noise. The deep fuzzy clustering algorithm reduces the impact of variations in dermoscopic images, hence resulting in better skin lesion segmentation. The pictorial comparison of the fuzzy based SegNet model and other conventional models is given in Figure 6.

Table 2. Output of the fuzzy based SegNet model and other conventional models

Models	ISIC-2017 dataset		ISIC-2017 dataset	
	Jaccard coefficient	Dice coefficient	Jaccard coefficient	Dice coefficient
K-means clustering	0.70	0.80	0.69	0.70
Fuzzy C means clustering	0.74	0.87	0.78	0.83
Superpixel clustering	0.80	0.88	0.87	0.86
U-Net	0.89	0.90	0.90	0.92
SegNet	0.94	0.95	0.95	0.95
Fuzzy based SegNet	0.98	0.99	0.97	0.98

As illustrated in Table 3, the classification performance of the normalized stacked LSTM network is compared with five traditional classification models namely, artificial neural network (ANN), recurrent neural network (RNN), gated recurrent unit (GRU), Bi-directional LSTM (Bi-LSTM), and stacked LSTM on the ISIC-2017 and PH2 datasets. As depicted in Table 3, the normalized stacked LSTM network obtains impressive classification results with 98.98% and 98.97% of accuracy correspondingly, on the ISIC-2017 and PH2 datasets, and these outcomes are significantly higher than those of the traditional classification models. Moreover, the normalized stacked LSTM network exhibits better results on other evaluation measures like sensitivity, precision, and MCC. The pictorial comparison of the normalized stacked LSTM network and other traditional classification models on the ISIC-2017 and PH2 datasets is correspondingly presented in Figures 7 and 8.

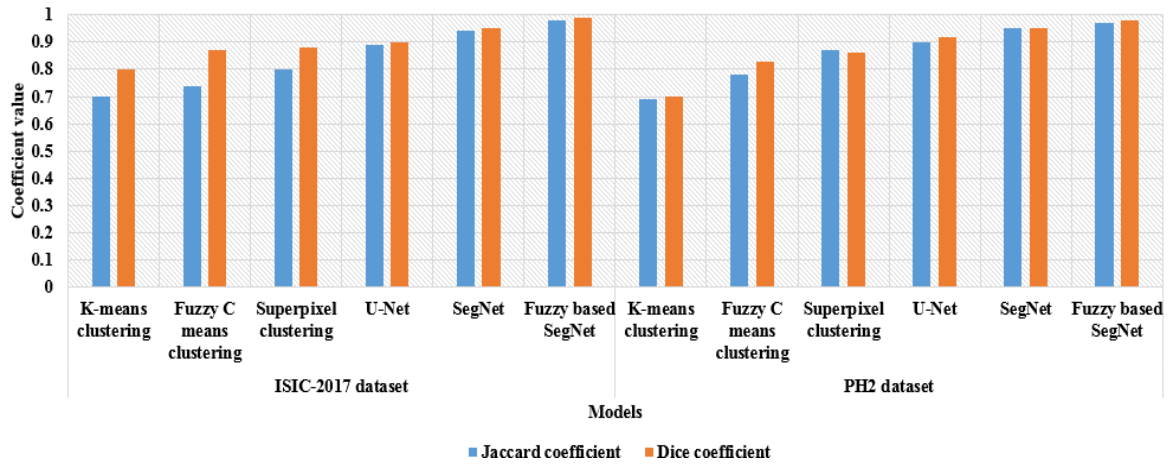


Figure 6. Pictorial comparison of the fuzzy based SegNet model and other conventional models

Table 3. Output of the normalized stacked LSTM network and other traditional classification models

ISIC-2017 dataset				
Models	Accuracy (%)	Sensitivity (%)	Precision (%)	MCC (%)
ANN	88.75	89.64	90.85	90.99
RNN	90.44	91.82	92.22	92.75
GRU	92.96	93.90	93.08	93.95
Bi-LSTM	95.54	94.85	96.52	94.77
Stacked LSTM	96.80	96.08	97.11	96.30
Normalized stacked LSTM	98.98	98.75	98.62	98.44
PH2 dataset				
Models	Accuracy (%)	Sensitivity (%)	Precision (%)	MCC (%)
ANN	92.80	94.90	92.11	90.28
RNN	93.22	95.28	93.88	93.54
GRU	93.98	96.44	94.65	96.55
Bi-LSTM	95.50	97.08	96.60	96.76
Stacked LSTM	97.66	97.87	97.96	97.88
Normalized stacked LSTM	98.97	98.55	98.76	98.90

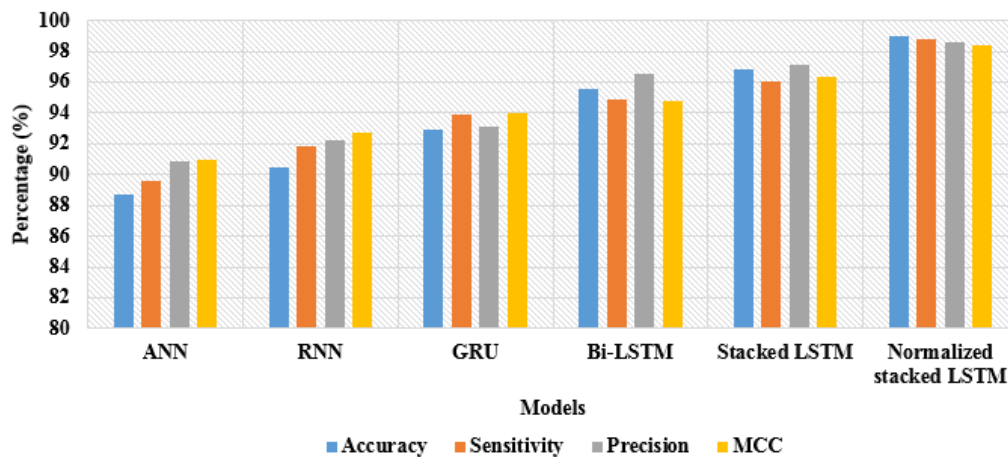


Figure 7. Pictorial comparison of the normalized stacked LSTM network and other traditional classification models on the ISIC-2017 dataset

In this classification segment, the traditional classification models (ANN, RNN, GRU, Bi-LSTM, and stacked LSTM) are executed in the same environment. The common parameters considered in these models are: dropout rate of 0.05, learning rate of 0.001, batch size of 64, activation functions are ReLU, sigmoid and tangent, total epochs of 100, and loss function is cross entropy. In comparison to the traditional

classification models, the normalized stacked LSTM model is effective in capturing longer-term spatial and temporal information from the extracted features, therefore resulting in better classification of dermoscopic images. The normalized stacked LSTM model efficiently classifies three classes, melanoma, seborrheic keratosis, and benign on the ISIC-2017 dataset, and three classes, melanoma, atypical nevi, and common nevi on the PH2 dataset.

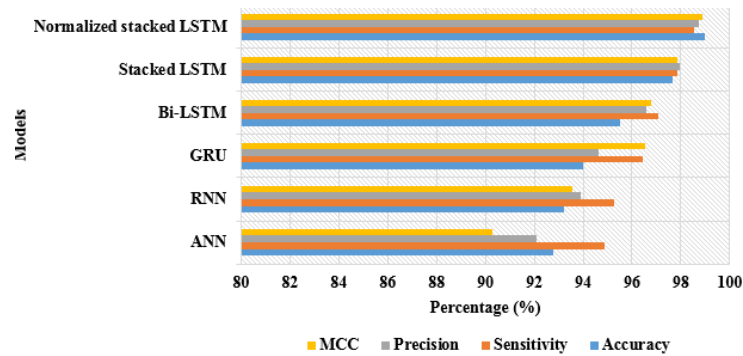


Figure 8. Pictorial comparison of the normalized stacked LSTM network and other traditional classification models on the PH2 dataset

Furthermore, the effectiveness of the normalized stacked LSTM model is analysed based on various K-fold cross validation techniques (K=2, 3, 5, and 8). By inspecting Table 4, it is evident that the normalized stacked LSTM model offers superior results in five-fold (20:80% testing and training) cross validation technique. The performing of cross validation reduces the risk of overfitting and bias by generalizing the proposed model on dissimilar subsets of image data.

Table 4. Outcomes of normalized stacked LSTM model on various K-fold cross validation techniques

Datasets	Measures (%)	K=2	K=3	K=5	K=8
ISIC-2017	Accuracy	96.50	96.40	98.98	97.55
	Sensitivity	96.12	95.39	98.75	96.06
	Precision	96.28	96.93	98.62	95.99
	MCC	97.36	95.72	98.44	95.77
PH2	Accuracy	96.58	96.68	98.97	96.92
	Sensitivity	97.68	95.27	98.55	97.64
	Precision	97.05	95.14	98.76	97.34
	MCC	96.80	95.44	98.90	97.62

### 3.3. Comparative analysis

The proposed automated system’s (combination of fuzzy based SegNet model and normalized stacked LSTM network) outcomes are compared with that of the existing systems developed by Araújo *et al.* [9], Ahmed *et al.* [10], Thanh *et al.* [11], and Goyal *et al.* [15]. Araújo *et al.* [9] which combined Link-Net and U-Net models for melanoma region segmentation. This hybrid model obtains 96.30% of accuracy, 90.50% of sensitivity, 0.92 of dice coefficient, and 0.85 of jaccard coefficient on the PH2 dataset. Ahmed *et al.* [10] combined mask RCNN and Retina-Net models for automatic MSC detection. This presented model obtains 93.20% of sensitivity, 0.92 of Jaccard coefficient, and 0.94 of dice coefficient on the PH2 dataset.

Furthermore, Thanh *et al.* [11] developed an efficient system for automatic MSC detection by employing different image processing techniques namely, APC, color normalization, and ABCD rule. The developed system achieves 96.60% of accuracy, 96.10% of sensitivity, 0.88 of Jaccard coefficient, and 0.93 of dice coefficient on the ISIC-2017 dataset. Goyal *et al.* [15] implemented an automated system by ensemble of different deep learning models (DeeplabV3+ and mask RCNN) for accurate MSC detection. This ensemble model achieves 94.08% of accuracy, 89.93% of sensitivity, 0.79 of Jaccard coefficient, and 0.87 of dice coefficient on the ISIC-2017 dataset. Correspondingly, this model obtains 93.80% of accuracy, 98.70% of sensitivity, 0.83 of Jaccard coefficient, and 0.90 of dice coefficient on the PH2 dataset. As mentioned in Table 5, in comparison to these existing systems, the proposed system attains significant detection performance, especially in the context of MSC.

Table 5. Comparative evaluation of the proposed system and other compared systems

Models	Dataset	Accuracy (%)	Sensitivity (%)	Dice coefficient	Jaccard coefficient
Link-Net and U-Net [9]	PH2	96.30	90.50	0.92	0.85
Mask RCNN and Retina-Net [10]	PH2	-	93.20	0.94	0.92
APC and ABCD rule [11]	ISIC-2017	96.60	96.10	0.93	0.88
DeeplabV3+ and mask RCNN [15]	ISIC-2017	94.08	89.93	0.87	0.79
	PH2	93.80	98.70	0.90	0.83
Fuzzy based SegNet model and normalized stacked LSTM network	ISIC-2017	98.98	98.75	0.99	0.98
	PH2	98.97	98.55	0.98	0.97

### 3.4. Discussion

Even though the modern research methods are effective in identifying and detecting skin cancer, it is very challenging due to a higher level of color similarity between melanoma non-affected areas and affected areas, and a lower contrast between the skin portions and melanoma moles. In the application of medical imaging, an automated system (combination of fuzzy based SegNet model, hybrid feature extraction, and normalized stacked LSTM network) is proposed for MSC detection. The deep fuzzy clustering algorithm is computationally effective because of the reusing of pooling indices, and this procedure removes the need of learning to perform upsampling. Additionally, the extraction of deep features by integrating ResNet-50 model and LTriDP descriptor decreases the semantic gap among features, thereby resulting in superior skin lesion classification. In the presented normalized stacked LSTM network, the layer normalization normalizes the activations in every layer of the LSTM network. This process reduces the overfitting risk and prevents this network from being sensitive to input patterns. By analyzing the simulation outcomes, it is learnt that still, the normalized stacked LSTM network has a problem of limited spatial understanding, and this is resolved by incorporating a spatial attention process as a future extension. This extension further improves the performance of this system for MSC detection. The normalized stacked LSTM network improves feature abstraction by learning hierarchical representations over temporal and spatial dimensions. This mechanism improves its generalization capability and facilitates precise classification.

## 4. CONCLUSION

In this manuscript, an efficient automated system is proposed for MSC detection by incorporating fuzzy based SegNet model and normalized stacked LSTM network. From the dermoscopic images acquired from ISIC-2017 and PH2 datasets, skin lesions are accurately segmented using a fuzzy based SegNet model. This segmentation model is more robust to noise and artefacts due to the incorporation of a deep fuzzy clustering algorithm. In addition, it is computationally effective due to the reuse of pooling indices in the SegNet model. The fuzzy based SegNet model incorporates the benefits of both deep fuzzy clustering algorithm and SegNet model, resulting in better segmentation performance related to other conventional models. The empirical analysis states that the fuzzy based SegNet model obtains 0.98 and 0.97 of jaccard coefficient, and 0.99 and 0.98 of dice coefficient on the ISIC-2017 and PH2 datasets, respectively. Furthermore, the normalized stacked LSTM network is proposed to categorize the classes of skin lesions. The normalized stacked LSTM network improves feature abstraction by learning hierarchical representations over temporal and spatial dimensions. This mechanism improves its generalization capability and facilitates precise classification. In comparison to other traditional classification models, the normalized stacked LSTM network obtains 98.98% and 98.97% of accuracy separately on the ISIC-2017 and PH2 datasets. By analyzing the simulation outcomes, it is learnt that still, the normalized stacked LSTM network has the problem of limited spatial understanding, and this is resolved by incorporating a spatial attention process as a future extension. This extension may further improve the performance of this system in MSC detection.

## REFERENCES

- [1] I. A. Alfi, M. M. Rahman, M. Shorfuazzaman, and A. Nazir, "A non-invasive interpretable diagnosis of melanoma skin cancer using deep learning and ensemble stacking of machine learning models," *Diagnostics*, vol. 12, no. 3, p. 726, Mar. 2022, doi: 10.3390/diagnostics12030726.
- [2] Q. Liu, H. Kawashima, and A. R. sofla, "An optimal method for melanoma detection from dermoscopy images using reinforcement learning and support vector machine optimized by enhanced fish migration optimization algorithm," *Heliyon*, vol. 9, no. 10, p. e21118, Oct. 2023, doi: 10.1016/j.heliyon.2023.e21118.
- [3] M. Shorfuazzaman, "An explainable stacked ensemble of deep learning models for improved melanoma skin cancer detection," *Multimedia Systems*, vol. 28, no. 4, pp. 1309–1323, Aug. 2022, doi: 10.1007/s00530-021-00787-5.
- [4] M. M. Rahman, M. K. Nasir, M. Nur-A-Alam, and M. S. I. Khan, "Proposing a hybrid technique of feature fusion and convolutional neural network for melanoma skin cancer detection," *Journal of Pathology Informatics*, vol. 14, p. 100341, 2023, doi: 10.1016/j.jpi.2023.100341.

- [5] N. Priyadharshini, S. N., B. Hemalatha, and C. Sureshkumar, "A novel hybrid extreme learning machine and teaching-learning-based optimization algorithm for skin cancer detection," *Healthcare Analytics*, vol. 3, p. 100161, Nov. 2023, doi: 10.1016/j.health.2023.100161.
- [6] P. Kavitha *et al.*, "Detection for melanoma skin cancer through ACCF, BPPF, and CLF techniques with machine learning approach," *BMC Bioinformatics*, vol. 24, no. 1, p. 458, Dec. 2023, doi: 10.1186/s12859-023-05584-7.
- [7] S. T. Sukanya and S. Jerine, "Skin lesion analysis towards melanoma detection using optimized deep learning network," *Multimedia Tools and Applications*, vol. 82, no. 18, pp. 27795–27817, Jul. 2023, doi: 10.1007/s11042-023-14454-6.
- [8] P. P. Tumpa and M. A. Kabir, "An artificial neural network based detection and classification of melanoma skin cancer using hybrid texture features," *Sensors International*, vol. 2, p. 100128, 2021, doi: 10.1016/j.sintl.2021.100128.
- [9] R. L. Araújo, F. H. D. de Araújo, and R. R. V. e Silva, "Automatic segmentation of melanoma skin cancer using transfer learning and fine-tuning," *Multimedia Systems*, vol. 28, no. 4, pp. 1239–1250, Aug. 2022, doi: 10.1007/s00530-021-00840-3.
- [10] N. Ahmed, X. Tan, and L. Ma, "A new method proposed to Melanoma-skin cancer lesion detection and segmentation based on hybrid convolutional neural network," *Multimedia Tools and Applications*, vol. 82, no. 8, pp. 11873–11896, Mar. 2023, doi: 10.1007/s11042-022-13618-0.
- [11] D. N. H. Thanh, V. B. S. Prasath, L. M. Hieu, and N. N. Hien, "Melanoma skin cancer detection method based on adaptive principal curvature, colour normalisation and feature extraction with the ABCD rule," *Journal of Digital Imaging*, vol. 33, no. 3, pp. 574–585, Jun. 2020, doi: 10.1007/s10278-019-00316-x.
- [12] M. Nawaz *et al.*, "Skin cancer detection from dermoscopic images using deep learning and fuzzy k -means clustering," *Microscopy Research and Technique*, vol. 85, no. 1, pp. 339–351, Jan. 2022, doi: 10.1002/jemt.23908.
- [13] T. Saba, "Computer vision for microscopic skin cancer diagnosis using handcrafted and non-handcrafted features," *Microscopy Research and Technique*, vol. 84, no. 6, pp. 1272–1283, Jun. 2021, doi: 10.1002/jemt.23686.
- [14] M. A. Al-masni, D.-H. Kim, and T.-S. Kim, "Multiple skin lesions diagnostics via integrated deep convolutional networks for segmentation and classification," *Computer Methods and Programs in Biomedicine*, vol. 190, p. 105351, Jul. 2020, doi: 10.1016/j.cmpb.2020.105351.
- [15] M. Goyal, A. Oakley, P. Bansal, D. Dancey, and M. H. Yap, "Skin lesion segmentation in dermoscopic images with ensemble deep learning methods," *IEEE Access*, vol. 8, pp. 4171–4181, 2020, doi: 10.1109/ACCESS.2019.2960504.
- [16] B. Cassidy, C. Kendrick, A. Brodzicki, J. Jaworek-Korjakowska, and M. H. Yap, "Analysis of the ISIC image datasets: usage, benchmarks and recommendations," *Medical Image Analysis*, vol. 75, p. 102305, Jan. 2022, doi: 10.1016/j.media.2021.102305.
- [17] H. K. Gajera, D. R. Nayak, and M. A. Zaveri, "A comprehensive analysis of dermoscopy images for melanoma detection via deep CNN features," *Biomedical Signal Processing and Control*, vol. 79, p. 104186, Jan. 2023, doi: 10.1016/j.bspc.2022.104186.
- [18] J. Sun *et al.*, "MASA-SegNet: a semantic segmentation network for PolSAR images," *Remote Sensing*, vol. 15, no. 14, p. 3662, Jul. 2023, doi: 10.3390/rs15143662.
- [19] R. Manickam, S. K. Rajan, C. Subramanian, A. Xavi, G. J. Enoch, and H. R. Yesudhas, "Person identification with aerial imagery using SegNet based semantic segmentation," *Earth Science Informatics*, vol. 13, no. 4, pp. 1293–1304, Dec. 2020, doi: 10.1007/s12145-020-00516-y.
- [20] L. Wen, X. Li, and L. Gao, "A transfer convolutional neural network for fault diagnosis based on ResNet-50," *Neural Computing and Applications*, vol. 32, no. 10, pp. 6111–6124, May 2020, doi: 10.1007/s00521-019-04097-w.
- [21] M. A. Ihsan Aquil and W. H. Wan Ishak, "Evaluation of scratch and pre-trained convolutional neural networks for the classification of Tomato plant diseases," *IAES International Journal of Artificial Intelligence (IJ-AI)*, vol. 10, no. 2, p. 467, Jun. 2021, doi: 10.11591/ijai.v10.i2.pp467-475.
- [22] H. Imaduddin, F. Yusfida Ala, A. Fatmawati, and B. A. Hermansyah, "Comparison of transfer learning method for COVID-19 detection using convolution neural network," *Bulletin of Electrical Engineering and Informatics*, vol. 11, no. 2, pp. 1091–1099, Apr. 2022, doi: 10.11591/eei.v11i2.3525.
- [23] M. Li, H. Wang, H. Liu, and Q. Meng, "Palmprint recognition based on the line feature local tri-directional patterns," *IET Biometrics*, vol. 11, no. 6, pp. 570–580, Nov. 2022, doi: 10.1049/bme2.12085.
- [24] E. Dandl and S. Karaca, "Detection of pseudo brain tumors via stacked LSTM neural networks using MR spectroscopy signals," *Biocybernetics and Biomedical Engineering*, vol. 41, no. 1, pp. 173–195, Jan. 2021, doi: 10.1016/j.bbe.2020.12.003.
- [25] D. Avola, M. Cascio, L. Cinque, G. L. Foresti, C. Massaroni, and E. Rodola, "2-D skeleton-based action recognition via two-branch stacked LSTM-RNNs," *IEEE Transactions on Multimedia*, vol. 22, no. 10, pp. 2481–2496, Oct. 2020, doi: 10.1109/TMM.2019.2960588.
- [26] H. Laaroussi, F. Guerouate, and M. Sbihi, "A novel hybrid deep learning approach for tourism demand forecasting," *International Journal of Electrical and Computer Engineering (IJECE)*, vol. 13, no. 2, p. 1989, Apr. 2023, doi: 10.11591/ijece.v13i2.pp1989-1996.
- [27] E. Alabdulkreem *et al.*, "Sustainable groundwater management using stacked LSTM with deep neural network," *Urban Climate*, vol. 49, p. 101469, May 2023, doi: 10.1016/j.uclim.2023.101469.
- [28] P. Rath, P. K. Mallick, H. K. Tripathy, and D. Mishra, "A tuned whale optimization-based stacked-LSTM network for digital image segmentation," *Arabian Journal for Science and Engineering*, vol. 48, no. 2, pp. 1735–1756, Feb. 2023, doi: 10.1007/s13369-022-06964-6.

## BIOGRAPHIES OF AUTHORS



**Woothukadu Thirumaran Chembian**    received the bachelor's degree in Electronics from the University of Madras, Tamil Nadu, India, in 1997, M.E Degree from Anna University, Chennai, Tamil Nadu, India in 2007 and Ph.D. in Computer Science and Engineering from Annamalai University, Chidambaram, Tamil Nadu, India in 2020. His research interest includes, image mining, neural networks, back propagation deep learning and artificial intelligence. From 2000 to 2020, he was worked various Anna University Affiliated Institutions. He is currently a full time Associate Professor in the Department of Computer Science and Engineering, Vel Tech High Tech Dr. Rangarajan Dr. Sakunthala Engineering College (Autonomous), 60, Avadi-Vel Tech Road Vel Nagar Avadi, Chennai, Tamil Nadu. He can be contacted at email: wtchembian@velhightech.com.



**Krishna Murthi Sankar**     is working as a Associate Professor in CVR College of Engineering in Hyderabad, Telangana. He Completed ME(CSE) in 2006 from Anna University and completed Ph.D. in 2013 from Anna University. He published 16 Scopus indexed journals and more than 20 non-indexed international journals. He has presented 20 International conferences and 25 national conferences. He wrote one book and one book chapter. He filed 4 patents. He is a Life Member in Computer Society of India (CSI), Mumbai, India and Life Member in Indian Society for Technical Education (ISTE), New Delhi India. He acted as a Placement Coordinator for the Students from 2007-2009, conducting various Training Programs for the students and placed the students in a reputable IT Company. He can be contacted at email: sankarkrish@cvr.ac.in.



**Seerangan Koteeswaran**     is currently working as Professor in the Department of Computer Science and Engineering (AI&ML), S.A. Engineering College, Chennai-600077, Tamil Nadu, India. He holds a Ph.D. Degree in Computer Science and Engineering from Vel Tech Rangarajan Dr. Sagunthala R&D Institute of Science and Technology. He is having 15 years of teaching experience and published more than 50 research articles in various peer reviewed Journals. He is author for two text books and two edited books for Computer Science and Engineering Programme. His research interests include artificial intelligence, machine learning, deep learning, big data and analytics and internet of things. He has presented several papers in conference proceedings. He is a reviewer for more than a dozen journals and also organized more than 25 various events such as National and International Conferences, Faculty Development Programs, Workshops, Seminars, National Level Paper Contests, Quiz programmes, 24 Hours IEEE Xtreme Programming Competition and 36 hours Hachathon. He is a Member of ACM, Member of IAEng, Global Member of ISOC, Member of IEEE CS, Member of IEEE CIS, Member of IEEE PCS, Member of IET, and a Senior Member of IEEE and also a Life Member of ISTE. He serves as Vice Chairman of ACM Chennai Chapter, Treasurer of IEEE Computer Society and Treasurer cum Secretary of IEEE Professional Communication Society, IEEE Madras Section and also served as Executive Committee Member, Chairman–Paper Contest and Vice Chairman–Student Activities Committee of IEEE Madras Section. He can be contacted at email: drkoteeswarans@saec.ac.in.



**Kandasamy Thinakaran**     received Ph.D. degree in computer science from Anna University, Tamil Nadu in 2017. He is currently working an Associate Professor in Computer Science Engineering, Saveetha School of Engineering, Chennai India. His current research interests include neural network and data mining. He can be contacted at email: thinakarank.sse@saveetha.com.



**Periyannan Raman**     is a Professor of Management Studies at Panimalar Engineering College, Chennai. He is an M.Com., MBA, M.Phil., and Ph.D., He has been teaching both Under graduate and Post graduate subjects for the last 25 years in the area of financial management, corporate finance, financial derivatives, merchant banking and financial services, investment management, economic analysis for business and accounting subjects. He has published six books in various titles and has presented papers in 20 International and 50 national seminars. He has also published papers in referred journals of repute. He can be contacted at email: raams.ram70@gmail.com.